Int. J. Electrochem. Sci., 12 **(2017)** 2088 – 2101, doi: 10.20964/2017.03.62

International Journal of
ELECTROCHEMICAL
SCIENCE
www.electrochemsci.org

Electrochemical and AFM Study of Inhibitory Properties of Thin Film Formed by Tartrazine Food Additive on 304L Stainless Steel in Saline Solution

Adriana Samide[1,*], *Gabriela Eugenia Iacobescu*[2,*], *Bogdan Tutunaru*[1], *Cristian Tigae*[1]

[1] University of Craiova, Faculty of Sciences, Department of Chemistry, Calea Bucuresti 107i, Craiova, Dolj, Romania
[2] University of Craiova, Faculty of Sciences, Department of Physics, A.I. Cuza, no.13, Craiova, Dolj, Romania
[*]E-mail: samide_adriana@yahoo.com; gabrielaiacobescu@yahoo.com

Received: 18 December 2016 / *Accepted:* 23 January 2017 / *Published:* 12 February 2017

Tartrazine, IUPAC name: Trisodium (4*E*)-5-oxo-1-(4-sulfonatophenyl)-4-[(4-sulfonatophenyl) hydrazono]-3-pyrazolecarboxylate, effect on the corrosion rate of 304L stainless steel used as canned food packaging has been studied by estimating the inhibitory properties of the organic film formed on the alloy surface during the electrochemical measurements performed in saline solution containing 0.9 % NaCl, without and with tartrazine inhibitor. AFM technique revealed the main surface changes of steel corroded in saline blank solution as well as in saline solution containing tartrazine food additive compared to standard stainless steel sample. A level of 92.8 % inhibition efficiency (*IE*) was reached for tartrazine inhibitor on 304L stainless steel corrosion in saline environment that involves a high degree of surface coverage at studied concentrations. Temkin adsorption model fitted well the experimental data, obtaining for the standard adsorption free energy (ΔG^{o}_{ads}) the value of -37.62 kJ mol^{-1}. Consequently gradual transition from physical adsorption to chemisorption takes place, and finally the moderate chemical adsorption prevails. The AFM parameters like: the values of the average roughness (R_a), RMS roughness (R_q) and maximum peak-to-valley height (R_{p-v}) showed that a smoother surface of 304L stainless steel was obtained in the tartrazine presence compared to that was observed in its absence, suggesting that the inhibitor film was formed on the alloy surface.

Keywords: Tartrazine; Inhibitory Coating; 304L Stainless Steel; Electrochemical Measurements; AFM.

1. INTRODUCTION

The development of certain systems for corrosion protection of the surface of materials in various environments has been a primordial objective for many investigations, which were aimed at

avoiding of irreversible damage to the metals and alloys. Due to the oxidation process, the metal surface may be affected in whole or in part, by the occurrence of local corrosion spots or areas where the pitting corrosion may be identified, and consequently certain properties of the material are modified. However, the corrosion products infest the environment emphasizing its pollution. Carbon steel and stainless steel are used the commonly in the manufacture of industrial equipments, such as pumps, blades for turbines, condensers etc. Moreover, 304L stainless steel is also used in the manufacture of food packaging for storage of food, such as canned. In this case, 304L stainless steel may be exposed to a systematic deterioration over time due to the characteristic action of salty environments, which can be accentuated and or contrary diminished by the presence of food additives. Many food additives can supplement the corrosion inhibitors through their ability to form coatings on the metal surface to inhibit subsequent oxidation processes. The inhibitors based on food additives can be used both for permanent protection and for temporary protection that involves the food storage timeshare.

Accordingly, many chemical compounds used as food additives have been investigated as corrosion inhibitors for different substrates in environment containing chloride ions. The acetic and benzoic acids are the most commonly acidity regulators. The corrosion behaviour of mild steel in aqueous acetic acid solution has been investigated by weight loss and electrochemical techniques [1, 2]. Also, it has been demonstrated that benzoic acid acts as corrosion inhibitor for iron and aluminium in 0.1 mol·L^{-1} NaCl solution [3].

Another category of food additives used in food industry is represented by anti-caking agents. The part of them used as corrosion inhibitors are carbonates [4], silicates [5, 6], stearic acid [7] and ferrocyanide [8] indicating good anti-corrosion properties for mild steel, stainless steel, iron and aluminium alloy in alkaline and acidic media in the presence of chloride ions. The inhibitive properties of food additives, as the antioxidants have been investigated, eg. vitamin C [9-13], vitamin B12 [14], vitamin E [15]. Vitamin C has been proved as an excellent inhibitor for the steel and copper corrosion in acid or alkaline media in the presence of chloride ions. The effect of vitamin B12 on mild steel corrosion in 0.5 mol L^{-1} H_2SO_4 has been studied by weight loss, potentiodynamic polarization and EIS measurements.

The β-carotene [16, 17] and uric acid [18] were also tested as corrosion inhibitors. Vitamin E and beta-carotene were investigated as green inhibitors for mild steel, copper, Cu-Zn and Cu-Al-Ni alloys in seawater, acid rain, sulfide and chloride solutions.

Bio-corrosion can develop simultaneously with the corrosion process due to the uncontrolled occurrence of the micro-organisms on some substrates that come into contact with different environments. Thus, a synergic effect of the two processes produces irreversible deterioration of the surfaces of materials with detrimental effects to the technical operation of industrial plants followed by economic damage. The attenuation of both processes can be simultaneously performed using certain substances that inhibit oxidation and the development of micro-organisms such as: moulds and bacteria. In this regard, the potassium sorbate was reported as an effective inhibitor for copper corrosion in aerated sulfate and chloride aqueous solutions [19]; sodium benzoate, potassium sorbate, sodium lauril-sulfate and p-aminobenzoate acid were investigated to reduce tinplate corrosion rate

[20]; an inhibition efficiency of 84 % was reported for steel corrosion in simulated carbonated solution containing chloride anions [21].

The determination of mild steel corrosion rate based on gravimetric, electrochemical and quantum chemical studies in hydrochloric acid solution, in the presence of food coloring additives have theoretical and practical importance. High inhibition efficiency was reported for Sunset Yellow, Amaranth, Allura Red, Tartrazine, Fast Green, Azorubine and Indigo Carmine food colorants [22-24].

Survey literature shows that food additives such as flavors are also efficient corrosion inhibitors for steel in aggressive media. Benzaldehyde (almond taste) and its derivatives [25], cinnamaldehyde (cinnamon taste) [26], limonene (orange taste) [27], ginger [28], eugenol [29], vanillin [30] were tested in the corrosion protection field.

The inhibition efficiency of sweeteners food additives such us; sodium saccharin [31], natural honey [32] and naturally occurring polysaccharides [33] have been reported to be very efficient corrosion inhibitors for steels in aggressive media.

The aim of the present study is to investigate the inhibitive properties of the tartrazine (FATTZ) known as E102 food coloring additive on the corrosion of 304L stainless steel in 0.9 % NaCl aqueous solution that generally is the saline environment of the canned food. The influence of inhibitor molecules on the electrode/electrolyte film formation was studied by potentiodynamic polarization followed by general corrosion test associated with Atomic Force Microscopy (AFM) technique to explore the surface morphology.

2. MATERIALS AND METHODS

2.1. Materials

The alloy of FeNi18Cr10 with the composition (wt %): C-0.03 %; Ni-18 %; Cr-10 %; Mn-2.0 %; Fe balance was used to cut the sheets with the area of 1.0 cm^2. These were subject to corrosion at room temperature and static regime, in saline solutions consisting in: 0.9 % NaCl blank solution and 0.9 % NaCl solution containing various concentrations of tartrazine: 0.2 mmol L^{-1}; 0.3 mmol L^{-1}; 0.4 mmol L^{-1}; 0.5 mmol L^{-1}. Bidistilled water was used for preparation of all solutions. All materials were purchased *via* a local supplier (Merk / Fluka / Sigma-Aldrich).

2.2. Electrochemical measurements

Electrochemical measurements were carried out at room temperature, in aerated and unstirred 0.9 % NaCl blank solution and 0.9 % NaCl solution containing various concentrations of FATTZ: 0.2 mmol L^{-1}; 0.3 mmol L^{-1}; 0.4 mmol L^{-1}; 0.5 mmol L^{-1}.

The electrochemical measurements implying the poteniodynamic polarization and the general corrosion tests of 304L stainless steel in uninhibited and inhibited with FATTZ of sodium chloride solutions were accomplished with a VoltaLab 40 electrochemical workstation, with VoltaMaster 4 software. A standard electrochemical cell was used having three electrodes coupled to electrochemical

workstation, VoltaLab, as follows: working electrode (304L stainless steel plates with area of 1.0 cm^2); counter electrode (platinum foil with area of 1.0 cm^2); Ag/AgCl, as reference electrode.

Before the potentiodynamic polarization, the steel plates used as working electrode were mechanically abraded with emery paper of different sizes, then ultrasonically degreased with ethanol, dried and kept under vacuum, at room temperature.

The polarization curves were recorded with the potential scan rate of 1.0 mV s^{-1}, after immersion time of electrodes in corrosive media of 4.0 min., it representing the potential stabilization time of the electrodes at open circuit. These were processed as Tafel semilogarithmic plots, in potential range of ± 250 mV reporting to the corrosion potential (E_{corr}), as well as Stern lines in potential domain close to E_{corr} (± 20 mV).

The general corrosion tests were performed after potentiodynamic polarization by recording the polarization resistance (R_p) values at every 72 s, time of 600 s, monitoring the changes that may occur at the metal/electrolyte interface, in the absence and in the presence FATTZ inhibitor. The polarization resistance (R_p) values were calculated using the "*General Corrosion"* option of VoltaMaster 4 software, which records step by step from 72 to 72 seconds, the polarization curves in the potential range close to corrosion potential. Thus, temporally computing of *R*p values are done by the Stern processing of the polarization curves.

2.3. Atomic Force Microscopy (AFM) measurements

Surface morphologies of the samples were observed by non-contact mode atomic force microscopy (NC-AFM, PARK XE-100 SPM system). The cantilever had a nominal length of 125 mm, a nominal force constant of 40 N/m, and oscillation frequencies in the range of 275–373 kHz. We used horizontal line by line flattening as planarization method. Average roughness (R_a), root-mean-square (RMS) roughness (R_q) and maximum peak to valley height (R_{p-v}) of the surfaces were estimated over the areas of 45×45 μm^2.

3. RESULTS AND DISCUSSION

3.1. Potentiodynamic polarization

3.1.1. Tafel processing

The potentiodynamic curves were recorded for 304L stainless steel, between -1000 mV and 100 mV, in saline solution without and with different concentations of FATTZ. After their processing as Tafel diagram in the potential range of ± 250 mV on both sides of corrosion potential (E_{corr}), the graph from Figure 1 was obtained. This shows that the addition of FATTZ leads to the slightly displacement of E_{corr} to higher values and in the same time, in lower current area, the curves were significantly moved. Consequently, FATTZ changes the characteristics of curves, acting prevalent on anodic process, the cathodic reaction being influenced up to -500 mV, when its rate was diminished.

At potential values under -500 mV, the cathodic process is less diminished, the curves being very close to that obtained in the blank solution. As shown Fig. 1, the values of FATTZ concentrations used for the inhibitor testing not significantly affect the anodic and the cathodic processes, the polarization curves are easily displaced relative to one another; the corrosion current density (i_{corr}) is not considerable modified with increase of FATTZ concentration (Table 1) and, as consequence the inhibition efficiency has about the same value, around 90.0 % (Table 1).

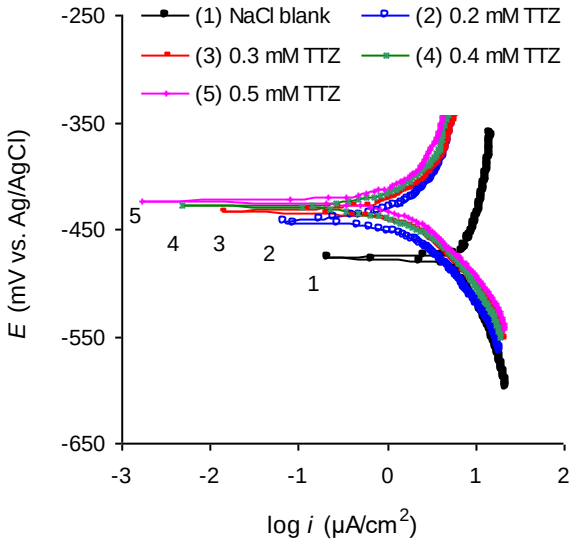

Figure 1. The potentiodynamic curves processed as Tafel diagram for 304L stainless steel corroded in 0.9 % NaCl solution, without and with FATTZ, at room temperature, after pre-polarizing time of electrodes at open circuit of 4.0 minutes

Thus, in the FATTZ concentration range of 0.2 - 0.5 mmol L^{-1}, the inhibition process of 304L stainless steel corrosion is significant, the FATTZ performance being very good considering its inhibition efficiency (*IE*), calculated with Expression 1 [22, 34-36], between 83.7-91.5 %, but it is less concentration-dependent.

$$IE = \frac{i^{o}_{corr} - i_{corr}}{i^{o}_{corr}} \times 100 \qquad (1)$$

where: i^{o}_{corr} and i_{corr} represent: the corrosion current density determined for 304L stainless steel corosion in 0.9 % NaCl blank solution and in 0.9 % NaCl solution containing various concentrations of tartrazine, respectively.

The values of Tafel slopes (Table 1) represent another indication of those previous notified, meaning that in the presence of the inhibitor, these have similar values, but different from those obtained in its absence (Table 1). All discussions lead to the conclusion that, the inhibition of 304L stainless steel corrosion in 0.9 % NaCl solution takes place because of metallic surface modification in the presence of tartrazine, that was adsorbed on the active sites forming an organic layer that enhances the inhibition process [37, 38], with the increase in FATTZ concentration. The electrochemical parameters listed in Table 1 were determined with VoltaMaster 4 software.

Table 1. Electrochemical parameteres and inhibition efficiency (IE %) obtained for 304L stainless steel corroded in 0.9 % NaCl solution, in the absence and in the presence of FATTZ inhibitor, under given laboratory conditions

C-FATTZ/ mmol L^{-1}	E_{corr}/ mV vs. Ag/AgCl	i_{corr}/ µA cm^{-2}	b_a/ mV dec^{-1}	b_c/ mV dec^{-1}	$C_p x10^3$/ $\Omega^{-1}cm^{-2}$	R_p/ Ω cm^2	IE (%)	
							Tafel	Stern
0	-476.5	31.7	159.6	-350.6	1.2813	780.4	-	-
0.2	-442.0	5.2	128.7	-217.2	0.1016	9842.5	83.7	92.1
0.3	-433.0	4.1	116.3	-214.4	0.1007	9930.4	87.1	92.1
0.4	-428.5	3.1	105.6	-207.9	0.0958	10438.4	90.2	92.5
0.5	-424.0	2.7	121.4	-210.7	0.0923	10834.2	91.5	92.8

3.1.2. Stern processing

Figure 2 illustrates the potentiodynamic curves processed as Stern diagram, in potential range near E_{corr}, apllying ± 20 mV on anodic and cathodic scans, respectively.

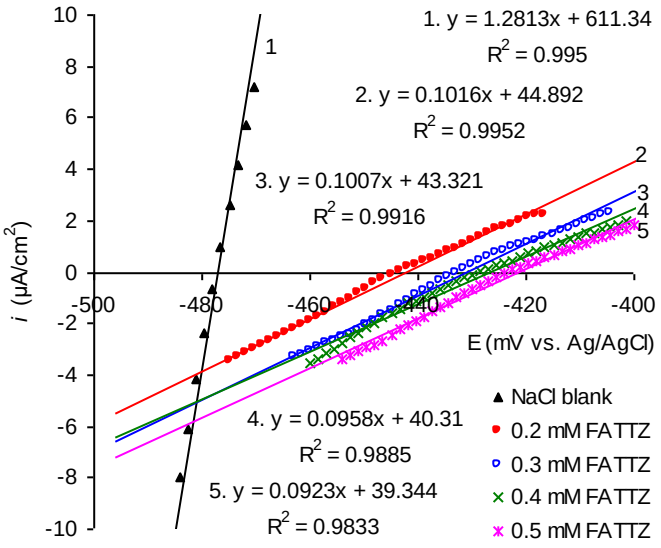

Figure 2. The potentiodynamic curves recorded close to corrosion potential in the range of ± 20 mV for 304L stainless steel corroded in 0.9 % NaCl solution, without and with FATTZ, at room temperature, after pre-polarizing time of electrodes at open circuit of 4.0 minutes

The polarization resistance was calculated with Relation 2 [39, 40], where polarization conductance (C_p) was determined from the slope of lines presented in Figure 2, as it has been reported in other studies, these are equl with $(di/dE)_{E\rightarrow Ecorr}$ [35, 39, 40]. Based on polarization rezistance (R_p), the inhibition efficiency (*IE*) was calculated with the relation 3 [34-36, 39].

$$C_p = 1/R_p \quad (2)$$

$$IE = \frac{R_p - R^o_p}{R_p} \times 100 \quad (3)$$

where: R^o_p is the polarization resistance obtained for 304L stainless steel in 0.9 % NaCl blank solution and R_p is the polarization resistance obtained for steel corrosion in 0.9 % NaCl solution containing investigated concentrations of FATTZ.

The data are centralized in Table 1 indicating the decrease of C_p, while the R_p and *IE* increse proportionally with the FATTZ concentration, the value of *IE* being about the same for all concentrations. Some previous studies have reported the tartrazine as corrosion inhibitor for zinc metal in 0.5 N H_2S0_4 solution [41] with a high efficiency around 85.0 % at 30 mmol L^{-1} of tartrazine concentration [41]. For the inhibition of mild steel corrosion in 0.5 mol L^{-1} HCl solution containing KI, the efficiency of tartrazine at 150 ppm concentration, was found about of 83.0 % [22].

As shown in Table 1 and Figure 2, the significant increase of R_p in the presence of FATTZ suggests a fundamental change of the composition of the metal surface due to the inhibitor adsorption with the development a film that blocks the corrosion process whose intensity is even lower with as the FATTZ concentration is higher, in saline solution. This behaviour was found for other food additives, e.g. vanillin. Its performance as corrosion inhibitor for aluminium, Al-Mg-Si alloy, stainless steel and carbon steel, in different media, was repoted in early investigations [30, 42-44].

As support for those stated, R_p was monitored over time for corroded 304L stainless steel in saline solution with and without inhibitor. A specific chart was recorded (Figure 3), which shows a sinusoidal variation of R_p in the absence of inhibitor and almost a constant value in its presence, especially at high concentrations, indicating a good stability of the FATTZ film adsorbed on surface [37, 45].

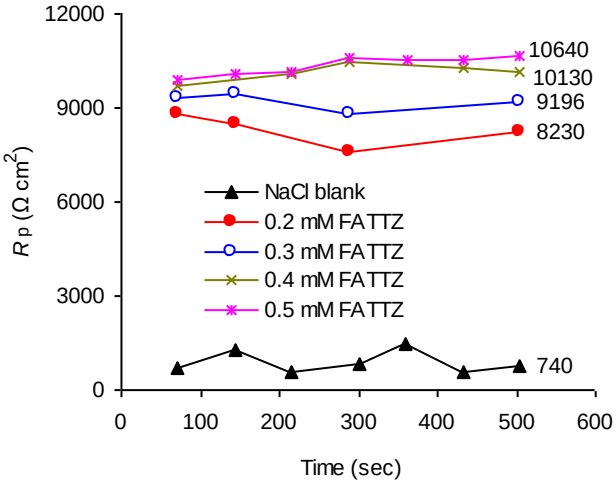

Figure 3. Variation of R_p over time monitored after potentiodynamic polarization of 304L stainless steel in saline solution; near each line drawn for inhibitor concentration, the R_p values at final moment are written

The same trend of R_p is observed, meaning that this increases with FATTZ concentration in the saline solution and at monitoring endpoint, values are slightly lower than those obtained from Stern chart (Table 1). This can be interpreted in terms of maintaining of inhibitor film stability, by its binding relatively strong to metal surface; thus, the tartrazine has blocked the active sites and/or this has participated to formation of complexes that improve the performance of protective coating from the steel surface [22].

3.2. Adsorption model approach

For the tested concentrations, it is difficult to simulate a model of FATTZ adsorption on the 304L stainless steel surface, because the values of inhibition efficiency (*IE*) exceed 80 %, that involves a surface coverage degree (θ), calculated as IE/100 [37, 39], higher than 0.8, when an isothermal approach is not indicated, in this case the linearization being uncertain.

Thus, the graph representing variation of surface coverage degree (θ) in function of inhibitor concentration (*C*-FATTZ) shows that by fitting the experimental data, a logarithmic dependence was obtained (Figure 4a).

By use the equation inserted in Fig. 4a, it was determined the functional coverage degree of surface (θ_f) that coresponds to following functional concentrations (C_f): 0.01 mmol L^{-1}; 0.02 mmol L^{-1}; 0.03 mmol L^{-1}; 0.04 mmol L^{-1}; 0.06 mmol L^{-1}; 0.08 mmol L^{-1}.

Moreover, the θ_f dependence of lnC_f is represented by a straight line that is shown in Figure 4b, it being characterized by the inserted equation. Thus, it was revealed the linearized form of Temkin adsorption isotherm expressed by the relation 4 [37, 39]:

$$\theta_f = \frac{1}{f} \cdot \ln K + \frac{1}{f} \cdot \ln C_f \qquad (4)$$

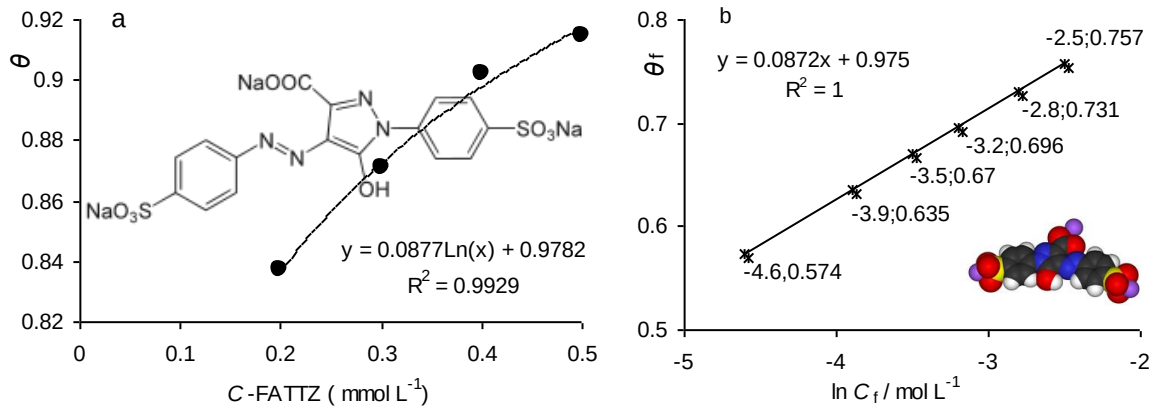

Figure 4. The molecular structure of tartrazine and the variation of surface coverage degree with the inhibitor concentration: a - fitting of the experimental data obtained under laboratory conditions; b - Temkin adsorption model for FATTZ inhibitor of 304L stainless steel corroded in 0.9 % NaCl solution

As shown in Figure 4b, *1/f* represents the line slope being equal with 0.0872, where *f* is associated with the number of active sites occupied by one inhibitor molecule [37, 39] reaching the value of 11.46. The intersection with the ordinate is represented by the expression [(1/*f*)·ln *K*], its value expressed in inserted equation from Fig. 4b is 0.975. This permits to calculate the adsorption-desorption equilibrium constant (*K*). Thus, for ln*K* was obtained the value of 11.1735 that was used to determine the standard adsorption free energy (ΔG^{o}_{ads}) by applying the relation 5 [34, 36, 39, 45-52].

$$\Delta G^{o}_{ads} = R \cdot T\,[\ln (1/55.5) - \ln K] \quad (5)$$

where: *K* represents the adsorption-desorption equilibrium constant; *R* is the universal constant of gases (8.31 J mol^{-1} K^{-1}), *T* is the temperature (298 K) and *55.5* is the value of the molar concentration of water in the solution.

The value obtained for ΔG^{o}_{ads} was negative (-37.62 kJ mol^{-1}), indicating a spontaneous adsorption process [37-41], mixed mechanism between physisorption and chemisorption being most likely and/or gradual transition from physical adsorption to chemical adsorption [38], that becomes predominant taking into account that ΔG^{o}_{ads} value is very close to -40.0 kJ mol^{-1} that represents the limit between physisorption and chemisorption [37, 39, 40, 45].

By analyzing of the tartrazine molecular structure (Fig. 4a), it can be seen that the inhibitor can bind to the steel surface by the lone pairs of electrons from nitrogen atoms of azo-group and the pyrazole cycle forming the coordinative bonds with metal cations from the electrical double layer. Compact arrangement of tartrazine molecule based on the optimized molecular formula observed in Fig. 4b allows the formation of uniform-distributed film with the metal-organic structure coherently-organized on the surface.

3.3. AFM observation

The effect of the inhibitor on the surface changes of 304L stainless steel corroded in 0.9 % NaCl solution may be discussed according to Atomic Force Microscopy (AFM), this being a technique which allows to study the surfaces at nano-level [53]. Also, by AFM the three-dimensional images can be obtained, which highlight the change in surface topography for the uncorroded and corroded samples in aggressive media in the absence and in the presence of the inhibitors [53].

The surface of the samples of 304L stainless steel before and after electrochemical measurements was analyzed by AFM; two-dimensional AFM images displaying the longitudinal-section and the three-dimensional images are illustrated in Figs. 5 and 6. Fig. 5 (a-c) present the 2D AFM images showing the longitudinal-section corresponding to uncorroded sample and corroded samples in 0.9 % NaCl solution without and with FATTZ. By AFM technique the roughness parameters were calculated and the corrosion process discussion was reported to their values. Average roughness (R_a), root-mean-square (RMS) roughness (R_q) and maximum peak to valley height (R_{p-v}) were commented in many studies which involve the corrosion inhibition process [53-56].

The values of the average roughness (R_a), RMS roughness (R_q) and maximum peak-to-valley height (R_{p-v}) for the 304L stainless steel surface before and after electrochemical measurements are listed in Table 2.

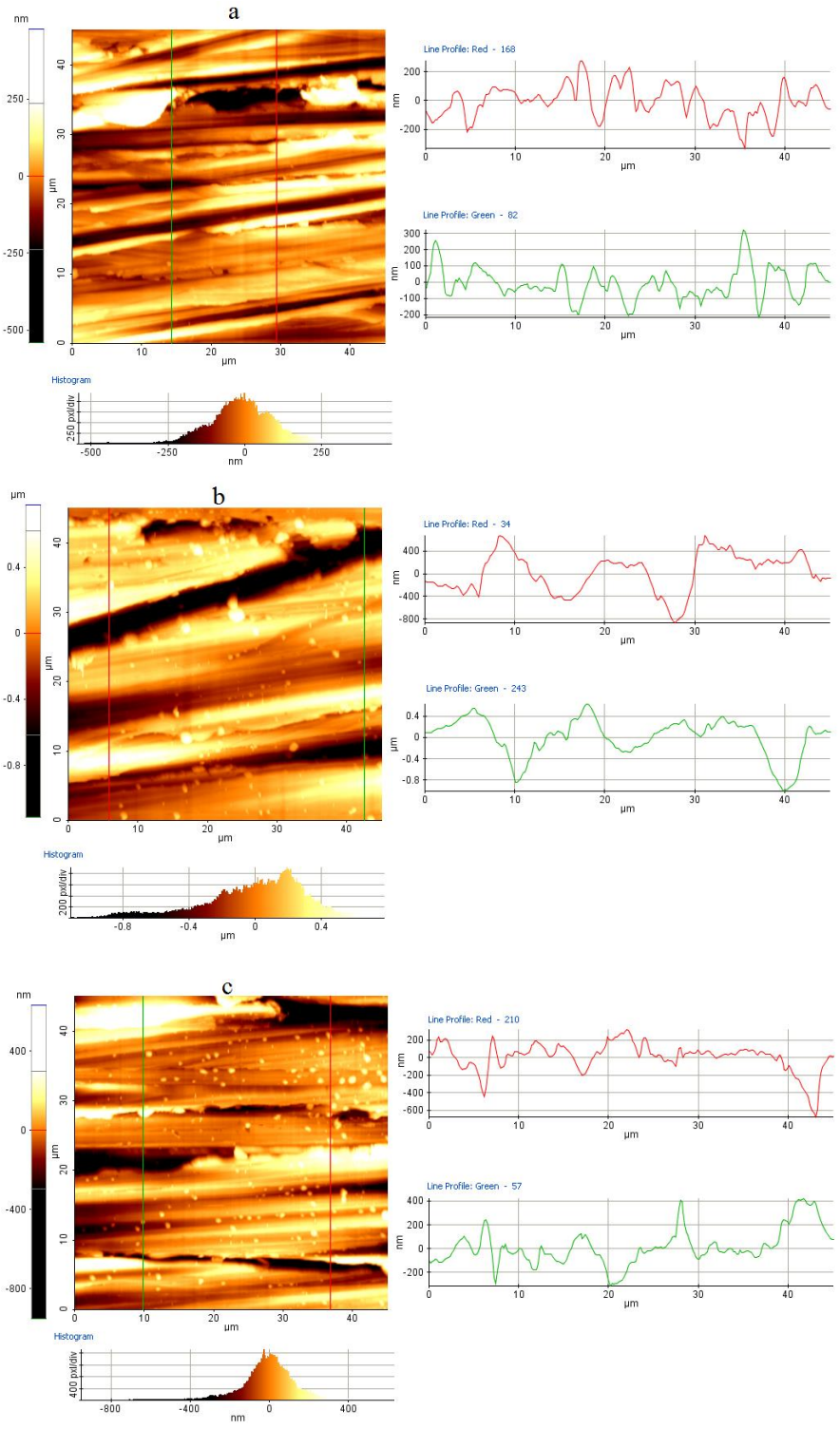

Figura 5. 2D AFM images and AFM logitudinal-sectional images of the 304L stainless steel surface: a - before corrosion (control sample); b - after corrosion in 0.9 % NaCl blank solution; c - after corrosion in 0.9 % NaCl solution containing 0.5 mmol L^{-1} FATTZ

As it is apparent from Table 2, R_a, R_q and $R_{p\text{-}v}$ follow the same trend for both lines red and green, meaning that these had the lowest values for the control sample, and the highest values were reached for the sample surface corroded in saline solution without inhibitor. The AFM results indicate

that the surface of 304L stainless steel corroded in 0.9 % NaCl solution without inhibitor is rougher, the surface roughness being due to the corrosion process [53-56].

Addition of FATTZ in saline solution leads to the change of steel surface AFM parameters. The values of R_a, R_q and R_{p-v} are significantly lower compared to those obtained for the steel surface corroded in uninhibited saline solution (Table 2). This decrease shows that the smoother surface [53] was obtained for the 304L stainless steel corroded in saline inhibited solution, suggesting that the protective film was formed by the tartrazine adsorption on the alloy surface [53, 56].

Table 2. AFM results obtained for 304L stainless corroded in saline blank solution and in saline blank solution containing 0.5 mmol L^{-1} FATTZ

Sample		R_q/ nm	R_a/ nm	R_{p-v}/ nm
SS control sample	Red line	113.2	89.9	609.8
	Green line	96.3	73.5	538.5
SS/NaCl	Red line	347	294	1541
	Green line	366	282	1645
SS/NaCl/FATTZ	Red line	167	115	993
	Green line	153	111	734

The 3D AFM images are displayed in Fig. 6 (a-c).

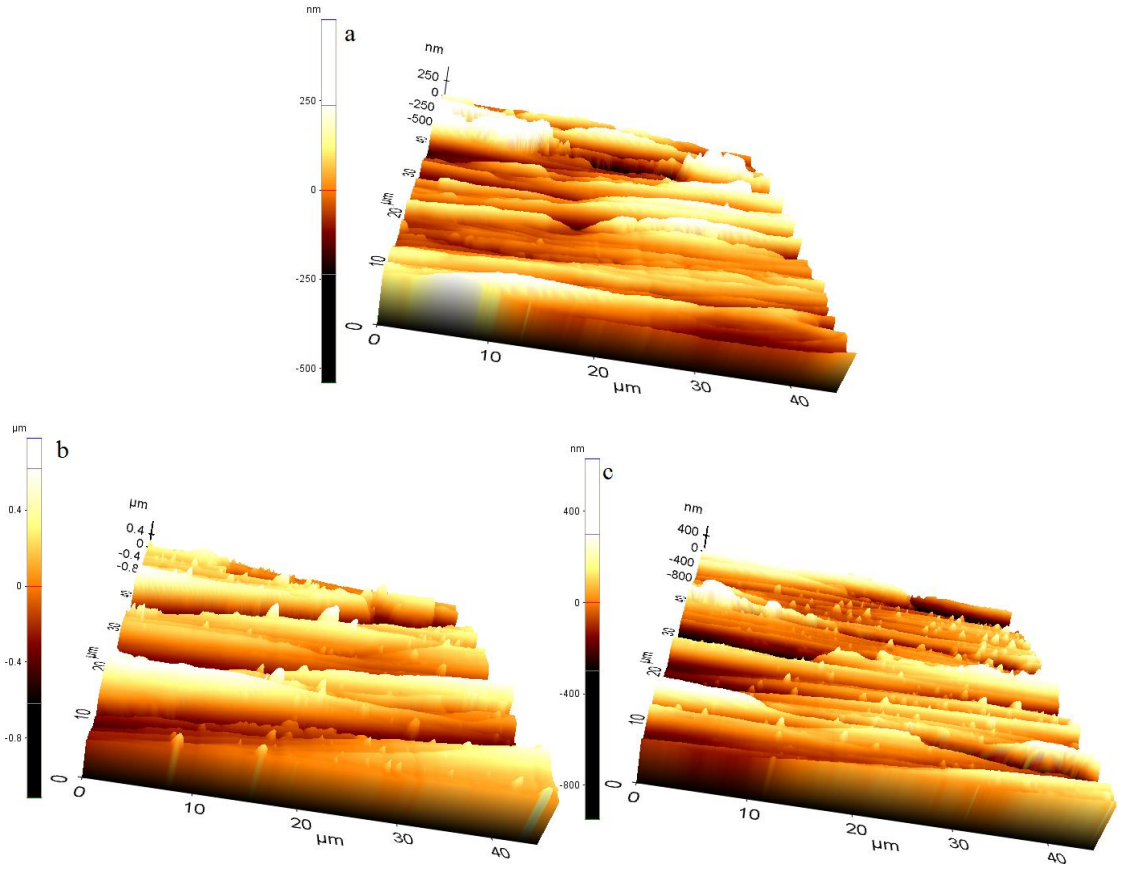

Figura 6. 3D AFM images of the 304L stainless steel surface: a - before corrosion (control sample); b - after corrosion in 0.9 % NaCl blank solution; c - after corrosion in 0.9 % NaCl solution containing 0.5 mmol L^{-1} FATTZ.

The Fig. 6a shows the surface of control sample is apparently uniform, the characteristics of smooth surface can be seen. The steel surface corroded in saline uninhibited solution (Fig. 6b) is uneven and covered with cone-like shapes of icicles formed from the salt crystals which randomly grew on the steel surface during corrosion process.

The corrosion pattern of the steel surface corroded in saline inhibited solution (Fig. 6c) is almost similar to that of uncorroded steel (Fig. 6a). It can be due to the inhibitor film formation through FATTZ adsorption. The difference consists in occurence of cone-like shapes of icicles on the surface, but these are smaller compared to those were observe in Fig. 6b.

Thus, it can be interpreted that the organic film formed by tartrazine adsorption on steel surface is doped with NaCl molecules and/or with Na^+ and Cl^- ions.

4. CONCLUSIONS

The electrochemical measurements were performed in order to determine the effect of tartrazine food additive on corrosion rate of 304L stainless steel in saline water containing 0.9 % NaCl, showing that, the corrosion current density sharply decreased starting with 0.2 mmol L^{-1} FATTZ and inhibition efficiency reached a high value about of 90.0 % in concentration range of 0.2-0.5 mmol L^{-1}.

Temkin adsorption isotherm was applied and the value of -37.62 kJ mol^{-1} for standard adsorption free energy (ΔG^o_{ads}) was calculated, that suggests a mixed adsorption mechanism between physisorption and chemisorption for tartrazine on 304L stainless steel surface.

The AFM parameters such as: the values of the average roughness (R_a), RMS roughness (R_q) and maximum peak-to-valley height (R_{p-v}) for the 304L stainless steel surface before and after electrochemical measurements indicated a different topography of alloy surfaces. The organic film formed by adsorption of tartrazine molecules on alloy surface was highlighted, in addition the protective coating has the insertions of NaCl molecules and/or Na^+ and Cl^- ions.

References

1. S. K. Singh, A. K. Mukherjee, M.M. Singh, *Indian J. Chem. Technol*. 18 (2011) 291.
2. S. K. Singh, A. K. Mukherjee, *J. Mater. Sci. Technol*. 26 (2010) 264.
3. S. Zor, *Turk J. Chem*. 26 (2002) 403.
4. C. Monticelli, M. Criado, S. Fajaro, J. M. Bastidas, M. Abbottoni, A. Balbo, *Cement Concrete Res*. 55 (2014) 49-58
5. Y. Xu, B. Lin, *Trans. Nonferrous Met. Soc*. China, 17 (2007) 1248.
6. O. Lopez-Garrity, G. S. Frankel, *Electrochim. Acta*, 130 (2014) 9.
7. X. Liu, S. Chen, H. Ma, G. Liu, L. Shen, *Appl. Surf. Sci*. 253 (2006) 814.
8. D. B. Hmamou, R. Salghi, A. Zarrouk, B. Hammouti, O. Benali, H. Zarrok, S. S. Al-Deyab, *Res. Chem. Intermed*. 39 (2013) 3475.
9. R. Fuchs-Godec, M. G. Pavlovic, M. V. Tomic, *Int. J. Electrochem. Sci*. 8 (2013) 1511.
10. R. Fuchs-Godec, M. G. Pavlovic, M. V. Tomic, *Int. J. Electrochem. Sci*. 10 (2015) 10502.
11. L. Valek, S. Martinez, M. Serdar, I. Stipanovic, *Chem Biochem. Eng. Q*., 21, 2007, 65-70.
12. M. A. Chidiebere, E. E. Oguzie, L. Liu, Y. Li, F. Wang, *J. Ind. Eng. Chem*. 26 (2015) 182.
13. M. A. Amin, *Chinese Chem. Lett*. 21 (2010) 341.
14. S. A. Kumar, A. Sankar, S.R. Kumar, *Int. J. Comput. Eng. Sci*. 3 (2013) 57.

15. R. Fuchs-Godec, G. Zerjav, *Corros. Sci*. 97 (2015) 7.
16. V. Sribharathy, S. Rajendran, J. Sathyabama, *Int. J. Chem. Sci. Technol*. 1 (2011) 108.
17. W. A. Badawy, M. M. El-Rabiei, *Chem. Mater. Res*. 6 (2014) 107.
18. Y. N. Prasad, S. Ramanathan, *Electrochim. Acta*, 52 (2007) 6353.
19. E. Abelev, D. Starosvetsky, Y. Ein-Eli, *Electrochim. Acta*, 52 (2007) 1975.
20. D.V. Taskovic, M.B. Rajkovic, D.D. Stanojevic, *J. Agr. Sci*., 50 (2005) 61.
21. F. Cao, J. Wei, J. Dong, W. Ke, *Corros. Sci*. 100 (2015) 365.
22. T. Peme, L.O. Olasunkanmi, I. Bahadur, A.S. Adekunle, M.M. Kabanda, E.E. Ebenso, *Molecules*, 20 (2015) 16004.
23. S.K. Shukla, A.K. Singh, L.C. Murulana, M.M. Kabanda, E.E. Ebenso, *Int. J. Electroch. Sci*. 7 (2012) 5057.
24. Z. Zhang. N. Tian, X. Li, L. Zhang, L. Wu, Y. Huang, *Appl. Surf. Sci*., 357 (2015) 845.
25. A. S. Fouda, M. M. Gouda, S. I. Abd El-Rahman, *Chem. Pharm. Bull*., 48 (2000) 636.
26. E. S. H. E. Ashry, A. E. Nemr, S. A. Essawy, S. Ragab, *Arkivoc*, XI (2006) 205.
27. E. Chaieb, A. Bouyanzer, B. Hammouti, M. Berrabah, *Acta Phys. - Chim. Sin*. 25 (2009) 1254.
28. A. Bouyanzer, B. Hammouti, *Bull. Electrochem*. 20 (2004) 63.
29. E. Chaieb, A. Bouyanzer, B. Hammouti, *Appl. Surf. Sci*., 246 (2005) 199.
30. A. Samide, B. Tutunaru, *J. Therm. Anal. Calorim*., 2016, DOI: 10.1007/s10973-016-5920-x.
31. A. L. Rose, A. P. P. Regis, S. Rajendran, F. R. S. Rani, *Int. Res. J. Pharm. App. Sci*., 3 (2013) 135.
32. A. Y. El-Etre, M. Abdallah, *Corros. Sci*. 42 (2000) 731.
33. S.A. Umoren, U.M. Eduok, *Carbohydrate Polymers*, 140 (2016) 314.
34. M. Scendo, J. Trela, *Int. J. Electrochem. Sci*., 8 (2013) 9201.
35. N. Ca1iskan, E. Akbas, *Mater. Chem. Phys.*, 126 (2011) 983.
36. A.S. Fouda, H.A. Mostafa, H.M. El-Abbasy, *J. Appl. Electrochem*., 40 (2010) 163.
37. A. Samide, B. Tutunaru, A. Moanţă, C. Ionescu, C. Tigae, A. C. Vladu, *Int. J. Electrochem. Sci*., 10 (2015) 4637.
38. F. M. Al-Nowaiser, *JKAU: Sci.*, 22 (2010) 89; Doi: I0.4197 *I* Sci. 22-2.7.
39. A. Samide, P. Rotaru, C. Ionescu, B. Tutunaru, A. Moanţă, V. Barragan-Montero, *J. Therm. Anal. Calorim*., 118 (2014) 651.
40. A. Samide, B. Tutunaru, A. Dobriţescu, P. Ilea, A. C. Vladu, C. Tigae, *Int. J. Electrochem. Sci*., 11 (2016) 5520.
41. A. Pasupathy, S. Nirmala, P. Sakthivel, G. Abirami, M. Raja, *Int. J. Scient. Res. Publications*, 4 (2014) 1.
42. A. Y. El-Etre, *Corros. Sci*., 43 (2001) 1031.
43. M. Shahidi, E. Sasaei, M. Ganjehkaviri, M. R. Gholamhosseinzadeh, *J. Phys. Theor. Chem*., 9 (2012) 149.
44. R. Rosliza, A. Nora'aini, W. B. Wan Nik, *J. Appl. Electrochem*., 40 (2010) 833.
45. A. Samide, B. Tutunaru, C. Ionescu, P. Rotaru, L. Simoiu, *J. Therm. Anal. Calorim*., 118 (2014) 118.
46. B. Zerga. A. Attayibat, M. Sfaira, M. Taleb, B. Hammouti, M. Ebn Touhami, S. Radi, Z. Rais, *J. Appl. Electrochem*., 40 (2010) 1575.
47. A. Samide, B. Tutunaru, *Cent. Eur. J. Chem*., 12 (2014) 901.
48. R. M. Hassan, I.A. Zaafarany, *Materials*, 6 (2013) 2436.
49. B. Zerga, B. Hammouti, M. Ebn Touhami, R. Touir, M. Taleb, M. Sfaira, M. Bennajeh, I. Forssal, *Int. J. Electrochem. Sci*., 7 (2012) 471.
50. M. Abdallah, I. Zaafarany, J.H. Al-Fahemi, Y.Abdallah, A.S. Fouda, *Int. J. Electrochem. Sci*., 7 (2012) 6622.
51. I. B. Obot, N. O. Obi-Egbedi, S.A. Umoren, *Corros. Sci*., 51 (2009) 1868.
52. M. Abdallah, I. Zaafarany, A. Fawzy, M.A. Radwan, E. Abdfattah, *J. Am. Sci*., 9 (2013) 580.
53. M. B. Geetha, B.S. Rajendran, *Der Pharma Chemica*, 8 (2016) 194.

54. H. Jafari, K. Akbarzade, I. Danaee, *Arab. J. Chem*. (2014) http://dx.doi.org/10.1016/j.arabjc.2014.11.018.
55. E. Q. Jasim, M. A. Mohammed-Ali, A. A. Hussain, *Chem. Mater. Res*. 7 (2015) 147.
56. C. M. Anbarasi, S. Rajendran, *Int. J. Current Eng. Tech*. 3 (2015) 2088.